Published in final edited form as:

Mol Cell Neurosci. 2017 April ; 80: 32–43. doi:10.1016/j.mcn.2017.01.008.

Molecular determinants of Cytochrome C oxidase IV mRNA axonal trafficking

Amar N. Kar[1], **Jose Norberto S. Vargas**[1], **Cai-Yun Chen**[1], **Jeffrey A Kowalak**[2], **Anthony E. Gioio**[1], and **Barry B. Kaplan**[1,*]

[1]Section on Neurobiology, Laboratory of Molecular Biology, Division of Intramural Research Programs, National Institute of Mental Health, National Institutes of Health, Bethesda, MD, USA

[2]NIMH-NINDS Clinical Proteomics Unit, Division of Intramural Research Programs, National Institute of Mental Health, National Institutes of Health, Bethesda, MD, USA

Abstract

In previous studies, we identified a putative 38-nucleotide stem-loop structure (zipcode) in the 3′ untranslated region of the cytochrome c oxidase subunit IV (COXIV) mRNA that was necessary and sufficient for the axonal localization of the message in primary superior cervical ganglion (SCG) neurons. However, little is known about the proteins that interact with the COXIV-zipcode and regulate the axonal trafficking and local translation of the COXIV message. To identify proteins involved in the axonal transport of the COXIV mRNA, we used the biotinylated 38-nucleotide COXIV RNA zipcode as bait in the affinity purification of COXIV zipcode binding proteins. Gel-shift assays of the biotinylated COXIV zipcode indicated that the putative stem-loop structure functions as a nucleation site for the formation of ribonucleoprotein complexes. Mass spectrometric analysis of the COXIV zipcode ribonucleoprotein complex led to the identification of a large number RNA binding proteins, including fused in sarcoma/translated in liposarcoma (FUS/TLS), and Y-box protein 1 (YB-1). Validation experiments, using western analyses, confirmed the presence of the candidate proteins in the COXIV zipcode affinity purified complexes obtained from SCG axons. Immunohistochemical studies show that FUS, and YB-1 are present in SCG axons. Importantly, RNA immunoprecipitation studies show that FUS, and YB-1 interact with endogenous axonal COXIV transcripts. siRNA-mediated downregulation of the candidate proteins FUS and YB-1 expression in the cell-bodies diminishes the levels of COXIV mRNA in the axon, suggesting functional roles for these proteins in the axonal trafficking of COXIV mRNA.

*Correspondence: Dr. Barry B. Kaplan, Section on Neurobiology, Laboratory of Molecular Biology, National Institute of Mental Health, National Institutes of Health, 49, Convent Drive, Room B1B80, Bethesda, MD 20892-4411, USA.

Supplementary Information:

1. Full List of specific proteins detected in Castello et al., 2012 and Fritzsche et al., 2013, as well as the non-specific proteins detected in these reports.
2. GO analyses results of RNP granule specific proteins identified in the this study as well as Castello et al., 2012, Fritzsche et al.2013, and Chu et al., 2015.

Keywords

Sympathetic neurons; mRNA trafficking; mRNA localization; RNA binding proteins; FUS; YB-1

Introduction

It is now evident that one of the mechanisms used by neurons to rapidly respond to developmental or extracellular cues is to temporally and spatially regulate protein expression by asymmetrical mRNA transport and translation (Jung et al., 2012; Gomes et al., 2014). Transcriptome analyses suggest the presence of a highly complex population of RNAs in axons, including messengers that encode proteins that can be organized into functional categories, such as cytoskeletal and scaffolding proteins, translation factors and ribosomal proteins, molecular motors and chaperones, and metabolic enzymes (Willis et al., 2007; Taylor et al., 2009; Zivraj et al., 2010). A major subset of mRNAs that localize to the axon encode mitochondrial proteins (Gumy et al., 2011; Ben-Yaakov et al., 2012; Merianda et al., 2013). These nuclear-encoded mitochondrial proteins are involved in the maintenance of organelle function and promote axonal survival (Gioio et al., 2001). Inhibition of local axonal mRNA translation or the import of mitochondrial proteins synthesized in the axon leads to decreases in mitochondrial membrane potential and the diminution of ATP synthesis in cultured neurons (Hillefors et al., 2007; Naranjo et al., 2012; Yoon et al., 2012). This finding suggests that the local synthesis and import of nuclear-encoded mitochondrial proteins to axonal mitochondria is essential to support the long-term viability and function of this distal structural domain of the neuron (for review, see Kaplan et al., 2009).

Interestingly, a number of these nuclear-encoded mitochondrial mRNAs code for proteins that play essential roles in oxidative phosphorylation. Studies on two such nuclear-encoded mitochondrial mRNAs, Cytochrome C oxidase IV (COXIV), and ATP synthase 9 (ATP5G1) that encode key subunits of oxidative phosphorylation complexes show that local translation of these mRNAs play an important role in the regulation of local axonal energy metabolism, as well as axon function and growth (Hillefors et al., 2007, Aschrafi et al., 2008, 2012; Natera-Naranjo et al., 2012). For example, disruption of the local translation of axonal COXIV or ATP5G1 mRNAs leads to compromised mitochondrial membrane potential, decreases in ATP levels and generation of reactive oxygen species (ROS) in the axon (Hillefors et al., 2007; Aschrafi et al., 2012; Natera-Naranjo et al., 2012).

Studies investigating cis-acting regulatory elements in COXIV mRNA that mediate the axonal trafficking of the transcript revealed a 38-nucleotide (nt) putative stem-loop structure (zipcode) in the 3′ untranslated region (3′UTR) that was necessary and sufficient to direct the localization of this message to the axon (Aschrafi et al., 2010). Overexpression of the COXIV zipcode in SCG neurons led to decreases in axonal ATP levels, elevated ROS production, as well as defects in axonal growth caused, at least in part, by the reduction in the levels of endogenous axonal COXIV mRNA (Aschrafi et al., 2010; Kar et al., 2014). These decrements in growth and axonal physiology could be partially rescued by decreasing axonal and mitochondrial ROS after application of antioxidants (Aschrafi et al., 2010). Interestingly, overexpression of the COXIV zipcode in select cortical regions of transgenic

animals showed increased neuronal ROS and the manifestation of aberrant behavioral phenotypes in young adults (Kar et al., 2014). Taken together, these findings suggest that the axonal transport of nuclear-encoded mitochondrial mRNAs plays an important role in basic neuronal function both *in vitro* and *in vivo.*

Selective mRNA transport and local translation of transcripts depends on the interaction of cis-acting regulatory elements in the transcript with RNA binding proteins to form ribonucleoprotein complexes (Doyle et al., 2012). However, little is known about the proteins that interact with the COXIV zipcode and mediate the trafficking of this transcript to the axon.

To identify the components of the COXIV zipcode ribonucleoprotein complex, we employed a RNA affinity pulldown-coupled mass spectrometry (MS)-based experimental approach. Our results show that the COXIV zipcode binding complex is enriched in RNA-binding proteins, as well as cytoskeletal and mitochondrial proteins. To evaluate the functional significance of the proteins identified by our proteomic approach we selected two candidate proteins: Fused in Sarcoma/Translocated in Sarcoma (FUS/TLS), and Y box binding protein 1(YB-1) for further analyses. These proteins have been previously shown to be involved in mRNA trafficking and translation (Lagier-Tourenne et al., 2010; Lyabin et al., 2014). Hence, these studies served as “proof of principle” experiments. Results of the RNA affinity purification, western blot analyses and siRNA-mediated knockdown experiments show that the COXIV zipcode indeed interacts with FUS, and YB-1 and that the expression of these proteins can modulate the transport of the COXIV transcript to the axon.

Experimental Procedures

Cell cultures

Superior cervical ganglions (SCG) neurons were cultured as described previously (Hillefors et al., 2007). Briefly, SCG were dissected from 3-day-old Harlan Sprague Dawley rat pups and were dissociated using the Miltenyi Biotec gentle MACS Dissociator and the Neuronal Tissue Dissociation Kit according to the manufacturer’s protocol. Dissociated primary neurons were plated into the center compartment of a three-compartmented Campenot culture chamber in serum-free Neurobasal medium (Invitrogen) containing nerve growth factor (NGF; 50 ng/ml; Alamone labs), 20 mM KCl, 20 U/ml penicillin and 20 mg/ml streptomycin (Hyclone) for 2–7 d. The culture medium was changed every 3–4 d. After 2 days-*in-vitro* (DIV), 5-fluoro-2′-deoxyuridine (FUDR, 50 μM) was added to the medium to inhibit the proliferation of non-neuronal cells. FUDR remained in the medium for the duration of the experiments. Media also contained nerve growth factor at all times. The side compartments, which contained the distal axons used in the experiments, were devoid of neuronal soma and non-neuronal cells, as judged by phase-contrast microscopy. For immunohistochemical studies, dissociated SCG neurons were plated on Nunc® Lab-Tek® II-CC2™ glass chamber slides (Sigma-Aldrich) pre-coated with collagen and grown for 1-week in culture before being processed for immunostaining.

SHSY5Y cells, a human dopaminergic clonal cell line, were maintained in F12: Dulbecco’s modified Eagle’s medium (DMEM) 1:1, supplemented with 10% fetal bovine serum, 100

units/mL Penicillin and 0.1 mg/mL streptomycin (Life Technologies). To foster differentiation, approximately 1×10^5 SHSY5Y cells were treated with 10 μM all-trans retinoic acid (RA) and 50 μg/mL NGF for 14 days in Neurobasal media supplemented with B27, GlutaMax, 100 units/mL Penicillin and 0.1 mg/mL streptomycin. Media was replaced every three days.

Cytosolic and Mitochondrial fraction preparation

Cytosolic extracts were prepared from 14-day-old RA-differentiated SHSY5Y cells or 2-week-old compartmentalized SCG cultures using the NE-PER™ Nuclear and Cytoplasmic Extraction Kit (Life Technologies) according to the manufacturer's instructions. The mitochondrial fractions were isolated from 2-week-old compartmentalized SCG cultures using the Mitochondria Isolation Kit for Cultured Cell according to the manufacturer's protocol. The cell-body and axonal compartments were processed separately. Protein concentration was determined using the Micro BCA Protein Assay Kit (Life Technologies).

Gel-shift assay

Cytosolic extracts were prepared from differentiated SHSY5Y cells as described earlier. Gel-shift assay was performed by incubating 10 μg of cytosolic extracts in binding buffer (20 mM HEPES, 72 mM potassium chloride, 1.5 mM magnesium chloride, 1.6 mM magnesium acetate, 0.5 mM dithiothreitol [DTT], 4 mM glycerol, 1 mM ATP, 200 units of RNasin; Promega) and 5 pmol of biotin-labelled oligonucleotides for 30 min at room temperature. For competition studies, the binding reactions were performed in the presence of 100-fold molar excess of non-biotinylated oligomer. After incubation, the reaction was fractionated by gel electrophoresis using 4% native polyacrylamide gels and 0.5 × TBE buffer (Biorad). The gel-shift bands were detected using the LightShift Chemiluminescent RNA electrophoretic mobility-shift assay (Life technologies) according to manufacturer's protocol.

RNA affinity purification

The experimental approach employed in the RNA affinity purification studies was based on a previous study with minor modifications (Kar et al., 2011). Biotinylated RNA oligonucleotides corresponding to the rat COXIV mRNA containing the last 38- and 22-nucleotides of the 3′ untranslated region were synthesized by *IDT technologies*. The 38nt oligomer is referred to as COXIV full-length zipcode, while the 22nt oligomer is called the 22nt deletion oligomer. For the RNA affinity pulldown experiments, 5 pmol of biotinylated RNA oligonucleotide was incubated in a reaction mixture (500μl) containing 100μl of differentiated SHSY5Y cytosolic extract in binding buffer (20mM HEPES/KOH (pH 7.9), 72mM potassium chloride, 1.5mM magnesium chloride, 1.625mM magnesium acetate, 0.5mM DTT, 4mM glycerol, 1mM ATP, 10ug E.coli tRNA), at room temperature for 30 min. After incubation, the RNA-protein mixtures are incubated with 100μl of magnetic streptavidin beads (Pierce Corporation) preequilibrated in binding buffer for 1 h at room temperature. After three washes with binding buffer, the bead-bound proteins were eluted by boiling for 10 min in elution buffer (125 mM Tris pH 6.8, 2% SDS, 0.02% bromophenol blue, 0.1M DTT) and size-fractionated by electrophoresis using a 4–12% gradient Bis-Tris SDS polyacrylamide gel (Life Technologies). The affinity purified proteins were visualized

by silver staining using the SilverQuest Staining Kit according to the manufacturer's instructions (Life Technologies).

Mass spectrometric analyses—For ultra-high pressure liquid chromatography – tandem mass spectrometry streptavidin bead-bound proteins were submitted to the NINDS/NIMH clinical proteomics core facility. The affinity purified proteins were processed using a modified version of a previously described on-bead digestion protocol (Berberich et al., 2011). The affinity purification and proteomic study was performed in quadruplets.

Data Analysis—Raw MS files were analyzed by PEAKS 7 search engine (build 20140312). PEAKS 7 uses MSFileReader (Thermo Scientific) to generate peak lists. MS/MS spectra were searched against a custom database constructed from the SwissProt portion of the UniProt database (release 2015_04). The database included all HUMAN sequences in SwissProt and was augmented with reagent protein sequences (LYSC_LYSEN, LYSC_PSEAE, SPA_STAA8, SPA_STAAU, SPG1_STRSG, SPG2_STRSG, and TRYP_PIG; 7,949 sequences). Search parameters used: precursor mass search type: monoisotopic, parent mass error tolerance: 10.0 ppm, fragment mass error tolerance: 0.6 Da, enzyme: trypsin, max missed cleavages: 2, non-specific cleavage: one (N-term or C-term), fixed modifications: carbamidomethylation (Cys), variable modifications: acetylation (Protein N-term), oxidation (Met), pyro-carbamidomethyl (camCys), pyro-Glu (Gln), max variable PTM per peptide: 3. The false discovery rate (FDR) was set to 0.01 for peptide-spectrum matches. For a protein to be reported to be present, at least two different peptide sequences were needed to be identified by the search algorithm that match this protein uniquely and should be present in at least 3 out of 4 the replicates analyzed.

To remove proteins that have been reported to be non-specific RNA binding proteins in the Btz, Stau2, Xist and RBPome studies, we had converted all the annotated proteins identified in each of the reports to human official gene symbols, using the bioDB ortholog gene conversion tool (https://biodbnet-abcc.ncifcrf.gov/db/dbOrthoRes.php). After conversion, the non-specific proteins lists were compared to COXIV zipcode granule component list to remove the non-specific binding proteins, using the Venn diagram generation webtool at Bioinformatics & Evolutionary Genomics (http://bioinformatics.psb.ugent.be/webtools/Venn/). This online tool identified all the non-specific binders that were identified in the COXIV zipcode granule mass spectroscopy results and these overlapping proteins were removed from the list of COXIV zipcode binding proteins. For generating the Venn diagrams comparing the proteins common between the COXIV zipcode study reported here and Btz, Stau2 and Xist studies, we again used the Venn diagram generation tool. Gene ontology (GO) term analysis was performed using DAVID (http://david.abcc.ncifcrf.gov). In DAVID, the following functional categories were analyzed for COXIV zipcode, Btz and Stau2, and Xist protein lists: biological pathway (BP), and cellular compartment (CC),

Transfection of neurons with small interfering RNA (siRNAs)

FUS- and YB-1-specific and non-targeting (NT)-siRNAs were purchased from Dharmacon. The siRNAs, each at final concentration of 100 pmoles, were transfected into cell-body or axonal compartments of 6–8-day-old Campenot cultures using Accell Transfection Systems

according to manufacturer's instructions (Life Technologies). Cell-bodies or axons, located in the central or lateral compartments of the chamber, were exposed to media containing the transfection reagents for 36 h.

Western blot analysis

Distal axons, were harvested and lysed in radioimmunoprecipitation assay (RIPA) buffer (Sigma Aldrich), containing complete protease inhibitor mixture (Roche). Equal amounts of each lysate were fractionated by 4–12% gradient SDS-PAGE and electroblotted onto 2-micron Nitrocellulose-based Transfer Membrane (Life Technologies). Membranes were blocked with ECL Advance Blocking Agent (GE Healthcare) for 1 h, followed by overnight incubation at 4°C with antibodies against either FUS (ProteinTech Group), YB-1 (Millipore), COXIV, β-actin (Cell Signaling Technology), and Tau (Sigma Aldrich) at 1:1000 dilution. Membranes were washed three times with 1 × TBS-Tween 20 (1 × TBS and 0.1% Tween 20) and incubated with HRP-labeled secondary antibody for 1 h at room temperature. After washing, membranes were developed with SuperSignal West Femto Maximum Sensitivity Substrate Detection Kit reagents (Life Technologies).

RNA isolation and quantitative reverse transcription polymerase chain reaction (qRT-PCR)

Total RNA was isolated from SCG axons or parental soma using Direct-Zol™ RNA MiniPrep (Zymo Research) according to the manufacturer's instructions. For reverse transcription, equal amounts of purified RNA were mixed with cDNA SuperMix (Quanta Biosciences™) and incubated in a Thermal Cycler (Life Technologies) for 5 min at 25 °C, followed by 30 min at 42 °C and 5 min at 85 °C. qRT-PCR analysis was performed with gene specific QuantiTect® primers (Qiagen) using VeriQuest SYBR Green Quantitative PCR Master Mix (Affymetrix). For each experimental RNA sample, the PCR reactions were run in triplicate, using a StepOne™ Real-Time PCR system (Applied Biosystems). The results were analyzed using the StepOne™ Software (Applied Biosystems), normalizing target mRNA levels to ribosomal protein subunit 18 (RPS18) or GAPDH mRNA levels.

RNA Immunoprecipitation (RNA-IP)

RNA immunoprecipitation experiments were performed on cytosolic extracts derived from either differentiated SHSY5Y cells, SCG distal axons or cell-bodies using FUS and YB-1 antibodies according to the protocol provided by the Magna RIP™ RNA-Binding Protein Immunoprecipitation Kit (Millipore). The immunoprecipitated RNA was subsequently analyzed by qRT-PCR. As negative control isotype-specific IgG pulldowns were performed. Also levels of GAPDH mRNA were used as a measure of non-specific RNA enrichment in the pulldown experiments. Enrichment was calculated as the ratio of the recovery of the target mRNA (COXIV) versus the recovery of the GAPDH negative control. Each experiment consisted of three biological replicates for each antibody pulldown and all experiments were performed three times.

Immunohistochemistry

Double immunostaining was carried out on 1-week-old dissociated SCG cultures using specific antibodies for FUS, YB-1, COXIV, ATP5G1 (Sigma Aldrich), and Tau. 1-week-old

dissociated SCG neurons were fixed for 10 min in prewarmed 4% paraformaldehyde solution and permeabilized using 0.5% Triton X-100 for 15 min. Cells were blocked in the blocking buffer (1× phosphate buffered saline [PBS] containing 3% bovine serum albumin [BSA] and 0.1% Triton X-100) at room temperature for 1 h and incubated with the antibodies at 4 °C overnight. After three washes with 1 × PBS, cells were incubated with the secondary antibodies at room temperature for 1 h and then processed for microscopy. Images were obtained using a confocal microscope (Zeiss LSM510).

Image analyses

ImageJ colocalization plugin was used to extract the overlapping immunohistochemical signals and JACoP plugin was used for the quantification of the colocalization.

Statistical analyses

All statistical analyses were performed in Excel. Results are expressed as mean ± standard error of the mean (SEM). Differences between groups were assessed with a Students' t-test (two groups), and one-way analysis of variance followed by post hoc tests for multiple group comparisons. p-values were calculated and a value less than 0.01 ($p \leq 0.01$) was considered significant.

Results

Identification of proteins binding to the COXIV 38nt zipcode

To identify the proteins that bind to the COXIV mRNA axonal localization element, we first employed a non-denaturing polyacrylamide gel-shift assay to test the hypothesis that the COXIV 38nt zipcode forms ribonucleoprotein complexes. Towards this end, cytosolic extracts prepared from 14-day-old retinoic acid-differentiated SHSY5Y neuroblastoma cells were incubated with biotinylated-RNA oligomer probes (see Materials and Methods). Indeed, the 38nt full-length COXIV zipcode forms stable RNA-protein complexes with proteins in the SHSY5Y extract (Fig. 1A, lane 2). However, the 22nt COXIV zipcode truncation, which does not promote axonal localization (Aschrafi et al., 2010), formed only weak complexes in the gel-shift assay (Fig. 1A, lane 3). The formation of the stable ribonucleoprotein complex after incubation of COXIV 38nt zipcode with SHSY5Y cell-lysate was specifically inhibited by the presence of the unlabeled (non-biotinylated) COXIV zipcode oligomer (Fig. 1B, compare lanes 2 and 3). Taken together, these data establish that the COXIV 38nt zipcode sequence has the capacity to form ribonucleoprotein complexes. Additionally, the marked reduction in the appearance of these complexes formed in the presence of the 22nt oligomer, employed as a negative control, as well as the depletion of the ribonucleoprotein complex upon competition with a non-biotinylated COXIV zipcode oligomer suggests that complex formation is not the result of non-specific nucleic acid/protein binding interactions.

Previous studies had shown that the targeting and local translation of the β-actin mRNA in specific sub-cellular compartments is regulated by the interaction of zipcode binding protein-1 (ZBP-1) with a 54-nucleotide cis-acting regulatory element located in the 3′UTR of the transcript (Ross et al., 1997; Zhang et al., 2001; Tiruchinapalli et al., 2003). To

ascertain whether ZBP-1 interacted with the COXIV 38nt zipcode, RNA affinity pulldown was performed followed by western analysis using a ZBP-1 specific antibody. As a positive control, a biotinylated 54nt β-actin RNA oligomer was used. The results show that as compared to the β-actin probe, which successfully affinity-purified ZBP-1, the COXIV 38nt zipcode showed no interaction with ZBP-1 (Fig. 1C). This result suggests that ZBP-1 is not a component of the RNP complex formed by the COXIV zipcode and raises the possibility that the RNP complexes containing the β-actin and COXIV mRNA zipcodes contain different sets of binding proteins.

To establish the identity of the proteins that interact with the COXIV 38nt zipcode, we used an RNA affinity purification-coupled mass spectrometry assay (see Fig. 2A). Briefly, the biotinylated COXIV 38nt zipcode RNA oligomer was incubated with SHSY5Y cytosolic extracts under conditions established previously in the gel-shift assay. After incubation, the ribonucleoprotein complexes were isolated by affinity pulldown using streptavidin-coated magnetic beads. The 22nt COXIV truncated probe as well as blank streptavidin beads were used as controls to exclude general nucleic acid RNA binding proteins and proteins that bound non-specifically to the streptavidin beads. Visualization of the affinity purified proteins by silver-staining of denaturing SDS-PAGE gels showed a variety of COXIV 38nt specific pulldown bands (Fig. 2B, compare lane 3 with lanes 1 and 2).

Mass spectrometry (MS) was employed to determine the identity of the protein components of the COXIV RNP complexes. In this experiment, 38nt COXIV oligomer- and 22nt deletion oligomer-specific RNA-protein complexes were bound to streptavidin beads and trypsin-digested. The peptides were subsequently separated and sequenced by liquid chromatography tandem mass spectrometry (LC-MS/MS). For a positive identification of a protein present in the affinity purified fraction at least two independent peptide sequences needed to be identified by the search algorithm that matched this protein uniquely (see Material and Methods). Proteins identified in the MS studies by virtue of single peptide hits were not included in the analysis. A list of COXIV zipcode and 22nt deletion associated proteins was generated after the analyses. This pairwise RNA-affinity pulldown and mass spectrometry analyses was performed four independent times. From the four experiments, a comprehensive lists of COXIV zipcode and 22nt deletion interacting proteins was generated. After comparing the lists of zipcode and deletion binding proteins for each replicate, approximately 87 proteins were identified that selectively bound to the COXIV 38nt zipcode. These 87 candidate COXIV zipcode-associated proteins were selected on the basis that they were either uniquely present in the COXIV full-length zipcode fraction or at least 1.5-fold enriched in three of the four COXIV full-length zipcode pulldowns. The enrichment of a protein in the COXIV zipcode fraction was defined as the presence of at least one or more unique peptides matching cognate protein in COXIV zipcode pulldown fraction as compared to the 22nt deletion oligomer. To eliminate proteins that may bind non-specifically to the magnetic streptavidin beads we compared our list of COXIV zipcode binding proteins with the list of proteins known to bind streptavidin beads as reported in the “bead proteome” study from the Lamond lab (Trinkle-Mulcahy et al., 2008), and removed the proteins that were common between the two studies. We next filtered our COXIV zipcode binding protein list by comparision with a list of non-specific protein interactors identified in the study reporting the isolation of proteins that comprise the Barentsz (Btz) and Staufen2 (Stau2)

ribonucleoparticle as reported by Fritzsche et al., 2013 and the non-specific background binders identified in the RNA binding protein interactome or RBPome studies (Castella et al., 2012) (Supplementary table I). The removal of the non-specific proteins identified in the aforementioned studies is highly relevant as the RNP isolating techniques used in these reports were similar to the one employed in our studies. After removing the non-specific binders from the list of 87 putative COXIV zipcode binding proteins, we identified approximately 53 candidate COXIV zipcode binders. A compilation of the putative COXIV zipcode-specific proteins isolated from the RNA affinity purification studies is provided in Table I.

Next we compared the protein components of the Stau2 (~65) and Btz RNP (~84), the *Xist* RNA granule (~82) (Chu et al., 2015) with the COXIV zipcode interacting proteins (for list of proteins see supplentary table I). The results show that only 3 proteins were common between the Btz and Stau2 and COXIV zipcode binders, while 12 proteins were common between Xist and COXIV zipcode interactors (Fig. 2C). This minimal overlap between the COXIV zipcode RNP and Btz, Stau2 and *Xist* RNA granule components provides evidence that COXIV zipcode is a part of a unique RNA/protein complex. To gain insight into the various functions of the identified proteins, we performed gene ontology (GO) term analysis using DAVID (Huang et al., 2009). This analysis revealed that five of the top twelve categories were related to RNA binding (see supplementary table II) as many of the identified proteins are known RBPs e.g., FUS, KHSRP, HNRNPA2B1, YBX1, HNRNPK. Importantly, however, a number of the identified RNA binding proteins have also been implicated in RNA trafficking e.g., HNRNPA3, RBM8A, KHSRP, FUS. This enrichment of RBPs is consistent with GO results obtained from BTz, Stau2 and *Xist* RNP granule components. Also consistent with the previous studies, we observed an enrichment of proteins such as, HMGB1, SEPT2, MAP4, CDK5, which are involved in processes such as neuron projection development and axon extension. Interestingly, unique to the COXIV zipcode RNA granule proteins, we observed an enrichment of proteins involved in biological processes, such as mitochondrion organization, mitochondrial electron transport and mitochondrial ATP synthesis. No such enrichment of mitochondrial-associated proteins were observed in either the Btz, Stau2 or the *Xist* studies (Supplementary table II). Consistent with the biological process enrichment results reported above, cell component-based clustering showed enrichment of proteins in broadly defined groups such as intracellular ribonucleoprotein complex, mitochondrion, axoneme, microtubule associated complex, and cytoplasmic stress granule etc. Taken together, the proteomic analysis show that the COXIV zipcode RNA granule contain unique RBP components distinct from other zipcode RNA granules.

To further evaluate the mass spectrometry results and explore the functional role of these proteins in the transport of COXIV mRNA to the axon, further studies were focused on two putative COXIV associated proteins: FUS/TLS, and YB-1. These candidate proteins were chosen based on their reported role in regulating mRNA processing and translation, as well as their possible involvement in the pathophysiology of neurodegenerative diseases (Lagier-Tourenne et al., 2010; Lyabin et al., 2014). To confirm the interaction of these proteins with the COXIV zipcode, RNA affinity purification experiments were performed. In these experiments, the biotinylated COXIV 38nt zipcode and 22nt deletion oligomer was

incubated with 2-wk-RA-differentiated SHSY5Y cytosolic lysates and the presence of FUS, and YB-1 in the complex was assessed by western analyses. As shown in Figure 3, the 38nt full-length COXIV zipcode oligomer binds both YB-1, and FUS (Fig. 3A and B). No interaction was observed between the 22nt-deletion oligomer and the two candidate proteins (Fig. 3A–B, compare lanes 1 and 2 lower panel). These results indicate that the COXIV zipcode RNP indeed contains YB-1, and FUS and serves to validate the results obtained from the mass spectrometry-coupled COXIV zipcode RNA affinity purifications.

COXIV mRNA interacts with zipcode-associating proteins in superior cervical ganglion neurons

To visualize the presence of the zipcode binding proteins in SCG neurons, we employed immunohistochemical analyses on 1-week-old dissociated SCG neurons that were cultured in collagen-coated glass chamber slides and stained with FUS-, and YB-1-specific antibodies. As shown in Figure 4, FUS, and YB-1 were present in the cell soma and axons of SCG neurons, as observed by the presence of FUS and YB-1 positive structures in axons stained with axonal marker Microtubule associated protein Tau. Co-staining immunohistochemical studies, using antibodies against mitochondrial proteins, COXIV and ATP5G1, showed partial overlap of YB-1 and FUS staining with these mitochondrial protein markers (Fig. 4A–B arrows). These results establish that the COXIV zipcode-interacting proteins FUS, and YB-1 are present in the axons and cell-bodies of SCG neurons and may interact with mitochondria in the axon.

To assess whether the COXIV zipcode interacts with FUS, and YB-1 in primary SCG neurons, RNA affinity purification experiments were performed using the 38nt full-length COXIV zipcode or the 22nt deletion oligomer, as bait in lysates derived from axons and cell-bodies of SCG neurons grown in Campenot compartmentalized cultures. We also evaluated the ability of the COXIV zipcode to assemble/form RNA granules in the axons by exposing the COXIV zipcode oligomer to axonal lysates isolated from distal axons located in the lateral compartments of Campenot chambers. Consistent with the results obtained using SHSY5Y cell-lysates, western blot analyses showed the presence of YB-1 and FUS in the COXIV zipcode purified fraction derived from cell-body and axonal extracts (Fig. 5A) and (Fig. 5B) respectively. The binding obtained with the full-length COXIV zipcode oligomer is specific as no signal was observed for any of the candidate proteins in the 22nt deletion oligomer purified fraction (Fig. 5A–B, compare lanes 2 and 3).

To test whether the endogenous FUS, and YB-1 protein present in the SHSY5Y cells interact with the COXIV transcript, we performed RNA immunoprecipitation (RIP) analyses. Briefly, FUS, and YB-1-specific antibodies were used to immunoprecipitate ribonucleoprotein complexes from cytosolic extracts derived from differentiated SHSY5Y cells. The presence of specific mRNA transcripts in these immunopurified fractions was assessed by reverse transcription polymerase chain reaction (RT-PCR) analyses using gene-specific primers. Agarose gel electrophoresis was performed to visualize the amplification products obtained from the RT-PCR reactions. As controls for this experiment, we used mouse and rabbit IgG and protein A/G beads to immunopurify COXIV mRNA. To control for enrichment of a highly abundant transcript via non-specific interaction during the

immunoprecipitation step, we used the highly abundant GAPDH mRNA as a negative control. Previous studies on both FUS and YB-1 did not reveal any evidence of interaction with the GAPDH mRNA (Masuda et al., 2015; Wu et al., 2015 respectively). Enrichment was calculated as the ratio of the recovery of the target mRNA (COXIV) versus the recovery of the GAPDH negative control. As shown in Figure 5C (upper panel), COXIV transcript PCR bands were obtained from RNA isolated from FUS, and YB-1-specific immunofractions (Fig. 5C upper panel, lanes 2–3). No COXIV-specific amplicons were obtained from RNA isolated from immunofractions derived from either rabbit or mouse IgG or the protein A/G beads alone (Fig. 5C upper panel, lanes 4–6). RT-PCR performed to test for the presence of GAPDH mRNA in the various immunofractions revealed non-specific binding of this transcript across all the immunopurified fractions (Fig. 5C lower panel lanes 2–6). No PCR amplicons were obtained with any of the primer sets tested in the minus-reverse transcriptase ("−RT") controls (data not shown). These results demonstrate a selective enrichment of COXIV mRNA in the FUS, and YB-1 immunopurified fractions, as compared to the either GAPDH transcript or the control mouse and rabbit IgG pulldown.

To validate the RNA-protein interactions observed in differentiated SHSY5Y cells in SCG neurons, we performed RIP followed by qRT-PCR on cell-body and axonal lysates obtained from SCG neurons grown in compartmentalized cultures. Similar to the data obtained from the SHSY5Y, RIP-qRT-PCR results revealed a significant enrichment of the COXIV transcript in the FUS, and YB-1 immunopurified fractions from SCG neurons relative to IgG or protein A/G bead pulldowns (Fig. 5D). In contrast, little enrichment was obtained for either GAPDH or β-actin gene transcripts used as negative controls. Consistent with the SCG neuron results, FUS, and YB-1 fractions obtained from brain lysates showed a specific enrichment of COXIV transcript as compared to the IgG pulldown (Fig. 5E). In contrast, no enrichment of the GAPDH transcript was observed in the candidate protein pulldowns. Overall, these results show that the COXIV zipcode interacting proteins, FUS, and YB-1 bind the endogenous COXIV transcript in cell-lines, primary sympathetic neurons, and rat brain.

siRNA-mediated downregulation of COXIV zipcode interacting protein expression leads to decreases in axonal COXIV mRNA levels in SCG neurons

The results of the previous experiments indicate that COXIV zipcode-interacting proteins FUS or YB-1 bind to COXIV mRNA. However, the functional significance of the interaction is unclear. To assess the significance of this binding on axonal COXIV mRNA levels, we performed siRNA-mediated knockdown of FUS or YB-1 expression in the cell-body and evaluated its effect on the levels of the COXIV mRNA. In this experiment, FUS- or YB-1-specific siRNAs were introduced into the cell-body compartment of the Campenot chambers (5–7 DIV) using the Accell siRNA transfection system. The transfection of non-targeting (NT−) siRNAs served as a negative control. Thirty-six hours after transfection, FUS and YB-1 mRNA and protein levels were assessed by qRT-PCR and western blot analyses, respectively. The results of these experiments showed that transfection of FUS-specific siRNA into the cell-body compartment of compartmentalized SCG cultures diminished FUS mRNA and protein levels by ~60–70% (Fig. 6A, B). A similar decrease in YB-1 mRNA and protein levels was also observed after transfection of YB-1 siRNA (Fig. 6A, B). No

diminution of FUS or YB-1 mRNA or protein levels were observed using NT-siRNA controls. Next, levels of axonal and cell-body COXIV mRNA and protein in SCG neurons were assessed by qRT-PCR and western analyses, after treatment of the cell-body compartment with FUS- or YB-1-specific siRNAs. SiRNA-mediated knockdown of cell-body FUS or YB-1 lead to a marked decrease in axonal COXIV transcript levels as compared with NT-siRNA-treated neurons (Fig. 6C). Consistent with the qRT-PCR results, western blot analyses of axonal lysates showed a marked decrease in COXIV protein levels as compared to non-targeting controls (Fig. 6D). These results indicate that cell-body levels of FUS and YB-1 proteins affect the levels of COXIV mRNA and protein in the axon. These findings raise the possibility that FUS and YB-1 may function to regulate the trafficking of COXIV mRNA to the axon.

Interestingly, analyses of cell-body COXIV mRNA levels revealed that YB-1-siRNA treatment led to a 60–70% decrease in COXIV transcript, while no significant alteration in COXIV levels was observed after FUS-siRNA treatment (Fig. 6C). However, a sharp increase in COXIV protein levels was observed in the cell-bodies treated with YB-1-specific siRNA. No significant change in COXIV protein levels in the cell-body was observed after FUS-siRNA treatment (Fig. 6D). These results suggest that, in addition to being a mediator of axonal trafficking, YB-1 may also function as a translational repressor of the COXIV transcript.

Discussion

The results provided in this communication indicate that a multi-protein ribonucleoprotein complex is formed in association with the COXIV 38nt zipcode. Evidence discussed below implicates components of this RNP in the regulation of the axonal localization of the COXIV transcript. The COXIV zipcode formed a RNP complex with cytosolic proteins derived from differentiated SHSY5Y cells in agarose gel-shift experiments, while no RNP complexes were observed with a COXIV 22nt fragment of the COXIV zipcode; a fragment which lacks the axonal localization activity. The complexes formed in association with the full-length (38nt) COXIV zipcode could be eliminated by competition with an excess of an unlabeled oligomer probe. The COXIV 38nt zipcode did not interact with ZBP-1, a protein known to be involved in the subcellular localization of several mRNAs (e.g. β-actin mRNA), a finding that indicates that not all zipcode trafficking complexes are comprised of identical sets of proteins.

RNA affinity purification experiments show that the 38nt COXIV zipcode was associated with several proteins in the cytosolic extracts, and this binding pattern was not observed with either the 22nt COXIV zipcode, or with a streptavidin bead negative control. Interestingly, minimal overlap was observed in the protein components identified to be present in the COXIV zipcode RNP and those reported to for the Btz, Stau2, *Xist* RNA granules, this observation suggests that zipcode trafficking complexes are heterogeneous in their composition. Previous studies have reported that RNA granules contain multiple RNA-binding proteins that function to stabilize and translationally silence the mRNA (Fritzsche et al., 2013; Chu et al., 2015). In addition, RNPs have also been shown to contain cytoskeletal proteins, which bind via adapters and motor proteins like Septins and Dyenins that regulate

the retrograde or anterograde transport of the complexes (Sotelo-Silveria et al., 2004, 2006, Donnelly et al., 2010; Tsang et al., 2011; Soundararajan et al., 2014). Consistent with these findings, our mass spectrometric analyses of the affinity purified COXIV zipcode-associated proteins revealed that a major proportion of the proteins forming COXIV zipcode RNP complex consist of RNA binding, as well as cytoskeletal proteins. One unique and highly specific feature revealed in our study was the presence of mitochondrial proteins in the COXIV zipcode affinity purified fraction. No such enrichment of mitochondria-associated protein complexes was observed in the previous RNA granule proteomic studies (Fritzsche et al., 2013; Chu et al., 2015). In support of our results, several mitochondrial proteins were indeed identified in a global screen for RNA binding proteins performed in HeLa cells, using the interactome capture methodology (Castello et al., 2012).

Biochemical and cell-biological studies were conducted on FUS, and YB-1 to validate the results of the RNA affinity purification experiments used to identify the COXIV zipcode binding proteins, as well as to evaluate the functional significance of the COXIV zipcode RNP in the axonal transport of the mRNA. These candidate proteins were selected based on prior studies showing their involvement in RNA processing including: transcription, splicing, transport and translation. For example, FUS is a RNA-binding protein that regulates the spatiotemporal fate of mRNA, i.e. subcellular localization, translation or degradation (de-Hoog et al., 2004; Fujii and Takumi, 2005; Andersson et al., 2008). Our results provide evidence that FUS interacts with the COXIV zipcode both in SHSY5Y cells and SCG neuronal cell-bodies and axons. In addition, the results of the RNA affinity pulldown experiments show that the FUS protein interacts with endogenous COXIV mRNA. Immunohistological studies conducted on primary sympathetic neurons show partial co-localization of FUS and mitochondrial proteins such as COXIV and ATP5G1, suggesting an association of FUS with mitochondria in the axon. Consistent with these results a recent report has shown that FUS interacts with mitochondrial proteins both in neuronal cultures and transgenic fly models (Deng et al., 2015). Knockdown of cell-body FUS expression leads to decreased axonal COXIV transcript levels in the absence of alterations in the cell-body levels of COXIV mRNA. This study is the first to report the role of FUS in the trafficking and or stability of nuclear-encoded mitochondrial mRNAs in the axon. Previous studies have shown that expression of ALS-associated FUS mutants lead to mitochondrial dysfunction, such as disorganized and fragmented mitochondrion in neurons (Huang et al., 2010, 2011; Tradwell et al., 2012; Deng et al., 2015). The findings reported in this study also provide a possible mechanism that may, in part, explain the mitochondrial abnormalities observed in mutant FUS expressing neurons.

In addition to FUS, it is also shown that COXIV mRNA interacts with YB-1 protein both in the axons and cell-bodies of sympathetic neurons and also notes the association of YB-1 with mitochondrial proteins in the axon. This is consistent with previous studies that showed that YB-1 interacts with mitochondria in mammalian cell culture systems (Matsumoto et al., 2012a, b). Importantly, knockdown of YB-1 in the cell-body of SCG neurons results in decreases in axonal levels of COXIV mRNA. Western blot analyses of COXIV protein levels in the axons after treatment with YB-1-specific siRNA revealed that, consistent with the decrease in axonal mRNA levels, COXIV protein levels in the axon are also reduced. Given the role of YB-1 in modulating both transcription and translation of nuclear-encoded

mitochondrial mRNAs (Matsumoto et al., 1989; Kohno et al., 2003; Matsumoto et al., 2012 a and b), the decrease in the COXIV transcript after YB-1 knockdown, could be explained by either a decrease in mRNA stability or decreased transcription of the COXIV gene. In the cell-body, we observe a reduction in COXIV mRNA levels after downregulation of YB-1 expression. However, western blot analyses revealed a spike in COXIV protein expression in the cell-body. This observation is consistent with a previous study that showed that siRNA-mediated downregulation of YB-1 leads to an increase in the relative abundance of a subset of proteins, including those involved in glycolysis, mitochondrial transport and oxidative phosphorylation (Somasekharan et al., 2012). Taken together, these data suggest that YB-1 may also function as a translational inhibitor and decreased YB-1 levels in the cell-body results in an upregulation of COXIV mRNA translation. It is also conceivable that the lack of YB-1 protein in the cell-body may inhibit the formation of COXIV trafficking granules, leading to decreased COXIV mRNA in the axon. Thus, this is the first study to call attention to the role of YB-1 in regulating both the transport and translation of nuclear-encoded mitochondrial transcripts in neurons.

In conclusion, using a proteomics-based approach, our studies have begun to provide a snapshot of the COXIV RNP complex that regulates the trafficking of the cognate transcript to the axon. We also report a novel function of FUS and YB-1 in the axonal trafficking and translation of COXIV mRNA. However, a detailed understanding of the molecular mechanisms by which FUS and YB-1 mediate its role in axonal trafficking and translation of COXIV transcript remains to be elucidated and experiments are underway towards that end. In addition, future studies will also focus on exploring the role of other candidate COXIV zipcode binding proteins identified by RNA affinity purification, such as KHSRP, hnRNPK, and NONO.

Supplementary Material

Refer to Web version on PubMed Central for supplementary material.

Abbreviations

COXIV	Cytochrome c oxidase subunit IV
SCG	Superior cervical ganglion
FUS/TLS	Fused in sarcoma/translated in liposarcoma
YB-1	Y-box protein 1
ATP5G1	ATP synthase 9
ROS	Reactive oxygen species
3′UTR	3′ untranslated region
ZBP-1	Zipcode binding protein-1
qRT-PCR	Quantitative reverse transcription polymerase chain reaction

RIP RNA immunoprecipitation

References

Andersson MK, Ståhlberg A, Arvidsson Y, Olofsson A, Semb H, Stenman G, Nilsson O, Aman P. The multifunctional FUS, EWS and TAF-15 proto-oncoproteins show cell type-specific expression patterns and involvement in cell spreading and stress response. BMC Cell Biol. 2008; 11(9):37.

Aschrafi A, Schwechter AD, Mameza MG, Natera-Naranjo O, Gioio AE, Kaplan BB. MicroRNA-338 regulates local cytochrome c oxidase IV mRNA levels and oxidative phosphorylation in the axons of sympathetic neurons. J Neurosci. 2008; 28:12581–90. [PubMed: 19020050]

Aschrafi A, Natera-Naranjo O, Gioio AE, Kaplan BB. Regulation of axonal trafficking of cytochrome c oxidase IV mRNA. Mol Cell Neurosci. 2010; 43:422–30. [PubMed: 20144716]

Aschrafi A, Kar AN, Natera-Naranjo O, Macgibeny MA, Gioio AE, Kaplan BB. MicroRNA-338 regulates the axonal expression of multiple nuclear-encoded mitochondrial mRNAs encoding subunits of the oxidative phosphorylation machinery. Cell Mol Life Sci. 2012; 69:4017–4027. [PubMed: 22773120]

Ben-Yaakov K, Dagan SY, Segal-Ruder Y, Shalem O, Vuppalanchi D, Willis DE, Yudin D, Rishal I, Rother F, Bader M, Blesch A, Pilpel Y, Twiss JL, Fainzilber M. Axonal transcription factors signal retrogradely in lesioned peripheral nerve. EMBO J. 2012; 31:1350–63. [PubMed: 22246183]

Berberich, MJ., Kowalak, JA., Makusky, AJ., Martin, D., Vullhorst, A., Buonanno, A., Markey, S. Development of an On-Bead Digestion Procedure for Immunoprecipitated Proteins in Sample Preparation in Biological Mass Spectrometry. Ivanov, AR., Lazarev, AV., editors. Springer Science +Business Media B.V.; 2011.

Castello A, Fischer B, Eichelbaum K, Horos R, Beckmann BM, Strein C, Davey NE, Humphreys DT, Preiss T, Steinmetz LM, Krijgsveld J, Hentze MW. Insights into RNA biology from an atlas of mammalian mRNA-binding proteins. Cell. 2012; 149(6):1393–406. [PubMed: 22658674]

Chu C, Zhang QC, da Rocha ST, Flynn RA, Bharadwaj M, Calabrese JM, Magnuson T, Heard E, Chang HY. Systematic discovery of Xist RNA binding proteins. Cell. 2015; 161(2):404–16. [PubMed: 25843628]

Deng J, Yang M, Chen Y, Chen X, Liu J, Sun S, Cheng H, Li Y, Bigio EH, Mesulam M, Xu Q, Du S, Fushimi K, Zhu L, Wu JY. FUS Interacts with HSP60 to Promote Mitochondrial Damage. PLoS Genet. 2015; 11(9):e1005357. [PubMed: 26335776]

Doyle M, Kiebler MA. A zipcode unzipped. Genes Dev. 2012; 26(2):110–3. [PubMed: 22279044]

Donnelly CJ, Fainzilber M, Twiss JL. Subcellular communication through RNA transport and localized protein synthesis. Traffic. 2010; 11:1498–505. [PubMed: 21040295]

Franceschini A, Szklarczyk D, Frankild S, Kuhn M, Simonovic M, Roth A, Lin J, Minguez P, Bork P, von Mering C, Jensen LJ. STRING v9.1: protein-protein interaction networks, with increased coverage and integration. Nucleic Acids Res. 2013; 41:D808–15. [PubMed: 23203871]

Fritzsche R, Karra D, Bennett KL, Ang FY, Heraud-Farlow JE, Tolino M, Doyle M, Bauer KE, Thomas S, Planyavsky M, Arn E, Bakosova A, Jungwirth K, Hörmann A, Palfi Z, Sandholzer J, Schwarz M, Macchi P, Colinge J, Superti-Furga G, Kiebler MA. Interactome of two diverse RNA granules links mRNA localization to translational repression in neurons. Cell Rep. 2013 Dec 26; 5(6):1749–62. [PubMed: 24360960]

Fujii R, Takumi T. TLS facilitates transport of mRNA encoding an actin-stabilizing protein to dendritic spines. J Cell Sci. 2005; 118(24):5755–65. [PubMed: 16317045]

Gioio AE, Eyman M, Zhang H, Lavina ZS, Giuditta A, Kaplan BB. Local synthesis of nuclear-encoded mitochondrial proteins in the presynaptic nerve terminal. J Neurosci Res. 2001; 64:447–53. [PubMed: 11391699]

Gumy LF, Yeo GS, Tung YC, Zivraj KH, Willis D, Coppola G, Lam BY, Twiss JL, Holt CE, Fawcett JW. Transcriptome analysis of embryonic and adult sensory axons reveals changes in mRNA repertoire localization. RNA. 2011; 17:85–98. [PubMed: 21098654]

Gomes C, Merianda TT, Lee SJ, Yoo S, Twiss JL. Molecular determinants of the axonal mRNA transcriptome. Dev Neurobiol. 2014; 74:218–32. [PubMed: 23959706]

Hillefors M, Gioio AE, Mameza MG, Kaplan BB. Axon viability and mitochondrial function are dependent on local protein synthesis in sympathetic neurons. Cell Mol Neurobiol. 2007; 27:701–16. [PubMed: 17619140]

de Hoog CL, Foster LJ, Mann M. RNA and RNA binding proteins participate in early stages of cell spreading through spreading initiation centers. Cell. 2004; 117(5):649–62. [PubMed: 15163412]

Huang DW, Sherman BT, Lempicki RA. Bioinformatics enrichment tools: paths toward the comprehensive functional analysis of large gene lists. Nucleic Acids Res. 2009; 37:1–13. [PubMed: 19033363]

Huang EJ, Zhang J, Geser F, Trojanowski JQ, Strober JB, Dickson DW, Brown RH Jr, Shapiro BE, Lomen-Hoerth C. Extensive FUS-immunoreactive pathology in juvenile amyotrophic lateral sclerosis with basophilic inclusions. Brain Pathol. 2010; 20:1069–76. [PubMed: 20579074]

Huang C, Zhou H, Tong J, Chen H, Liu YJ, Wang D, Wei X, Xia XG. FUS transgenic rats develop the phenotypes of amyotrophic lateral sclerosis and frontotemporal lobar degeneration. PLoS Genet. 2011; 7:e1002011. [PubMed: 21408206]

Jung H, Yoon BC, Holt CE. Axonal mRNA localization and local protein synthesis in nervous system assembly, maintenance and repair. Nat Rev Neurosci. 2012; 13:308–24. [PubMed: 22498899]

Kaplan BB, Gioio AE, Hillefors M, Aschrafi A. Axonal protein synthesis and the regulation of local mitochondrial function. Results Probl Cell Differ. 2009; 48:225–42. [PubMed: 19343315]

Kar A, Fushimi K, Zhou X, Ray P, Shi C, Chen X, Liu Z, Chen S, Wu JY. RNA helicase 68 (DDX5) regulates tau exon 10 splicing by modulating a stem-loop structure at the 5′ splice site. Mol Cell Biol. 2011; 31:1812–21. [PubMed: 21343338]

Kar AN, Sun CY, Reichard K, Gervasi NM, Pickel J, Nakazawa K, Gioio AE, Kaplan BB. Dysregulation of the axonal trafficking of nuclear-encoded mitochondrial mRNA alters neuronal mitochondrial activity and mouse behavior. Dev Neurobiol. 2014; 74:333–50. [PubMed: 24151253]

Kohno K, Izumi H, Uchiumi T, Ashizuka M, Kuwano M. The pleiotropic functions of the Y-box-binding protein, YB-1. Bioessays. 2003; 25:691–8. [PubMed: 12815724]

Lagier-Tourenne C, Polymenidou M, Cleveland DW. TDP-43 and FUS/TLS: emerging roles in RNA processing and neurodegeneration. Hum Mol Genet. 2010; 19:R46–64. [PubMed: 20400460]

Lyabin DN, Eliseeva IA, Ovchinnikov L. YB-1 protein: functions and regulation. Wiley Interdiscip Rev RNA. 2013; 5(1):95–110. [PubMed: 24217978]

Masuda A, Takeda J, Okuno T, Okamoto T, Ohkawara B, Ito M, Ishigak IS, Sobue G, Ohno K. Position-specific binding of FUS to nascent RNA regulates mRNA length. Genes Dev. 2015; 29(10):1045–57. [PubMed: 25995189]

Matsumoto K, Nagata K, Yamanaka K, Hanaoka F, Ui M. Nuclear factor I represses the reverse-oriented transcription from the adenovirus type 5 DNA terminus. Biochem Biophys Res Commun. 1989; 164:1212–9. [PubMed: 2480114]

Matsumoto S, Uchiumi T, Tanamachi H, Saito T, Yagi M, Takazaki S, Kanki T, Kang D. Ribonucleoprotein Y-box-binding protein-1 regulates mitochondrial oxidative phosphorylation (OXPHOS) protein expression after serum stimulation through binding to OXPHOS mRNA. Biochem J. 2012a; 443:573–84. [PubMed: 22280412]

Matsumoto S, Uchiumi T, Saito T, Yagi M, Takazaki S, Kanki T, Kang D. Localization of mRNAs encoding human mitochondrial oxidative phosphorylation proteins. Mitochondrion. 2012b; 12:391–8. [PubMed: 22406259]

Merianda TT, Vuppalanchi D, Yoo S, Blesch A, Twiss JL. Axonal transport of neural membrane protein 35 mRNA increases axon growth. J Cell Sci. 2013; 126:90–102. [PubMed: 23097042]

Natera-Naranjo O, Kar AN, Aschrafi A, Gervasi NM, Macgibeny MA, Gioio AE, Kaplan BB. Local translation of ATP synthase subunit 9 mRNA alters ATP levels and the production of ROS in the axon. Mol Cell Neurosci. 2012; 49:263–70. [PubMed: 22209705]

Ross AF, Oleynikov Y, Kislauskis EH, Taneja KL, Singer RH. Characterization of a beta-actin mRNA zipcode-binding protein. Mol Cell Biol. 1997; 17(4):2158–65. [PubMed: 9121465]

Somasekharan SP, Stoynov N, Rotblat B, Leprivier G, Galpin JD, Ahern CA, Foster LJ, Sorensen PH. Identification and quantification of newly synthesized proteins translationally regulated by YB-1 using a novel Click-SILAC approach. J Proteomics. 2012; 21(77):e1–10.

Sotelo-Silveira JR, Calliari A, Cárdenas M, Koenig E, Sotelo JR. Myosin Va and kinesin II motor proteins are concentrated in ribosomal domains (periaxoplasmic ribosomal plaques) of myelinated axons. J Neurobiol. 2004; 60:187–96. [PubMed: 15266650]

Sotelo-Silveira JR, Calliari A, Kun A, Koenig E, Sotelo JR. RNA trafficking in axons. Traffic. 2006; 7:508–15. [PubMed: 16643274]

Soundararajan HC, Bullock SL. The influence of dynein processivity control, MAPs, and microtubule ends on directional movement of a localising mRNA. Elife. 2014; 15(3):e01596.

Tradewell ML, Yu Z, Tibshirani M, Boulanger MC, Durham HD, Richard S. Arginine methylation by RMT1 regulates nuclear-cytoplasmic localization and toxicity of FUS/TLS harbouring ALS-linked mutations. Hum Mol Genet. 2012; 21:136–49. [PubMed: 21965298]

Taylor AM, Berchtold NC, Perreau VM, Tu CH, Li JN, Cotman CW. Axonal mRNA in uninjured and regenerating cortical mammalian axons. J Neurosci. 2009; 29:4697–707. [PubMed: 19369540]

Tiruchinapalli DM, Oleynikov Y, Kelic S, Shenoy SM, Hartley A, Stanton PK, Singer RH, Bassell GJ. Activity-dependent trafficking and dynamic localization of zipcode binding protein 1 and beta-actin mRNA in dendrites and spines of hippocampal neurons. J Neurosci. 2003; 23(8):3251–61. [PubMed: 12716932]

Trinkle-Mulcahy L, Boulon S, Lam YW, Urcia R, Boisvert FM, Vandermoere F, Morrice NA, Swift S, Rothbauer U, Leonhardt H, Lamond A. Identifying specific protein interaction partners using quantitative mass spectrometry and bead proteomes. J Cell Biol. 2008; 183(2):223–39. [PubMed: 18936248]

Tsang CW, Estey MP, DiCiccio JE, Xie H, Patterson D, Trimble WS. Characterization of presynaptic septin complexes in mammalian hippocampal neurons. Biol Chem. 2011; 392:739–49. [PubMed: 21767234]

Willis DE, van Niekerk EA, Sasaki Y, Mesngon M, Merianda TT, Williams GG, Kendall M, Smith DS, Bassell GJ, Twiss JL. Extracellular stimuli specifically regulate localized levels of individual neuronal mRNAs. J Cell Biol. 2007; 178:965–80. [PubMed: 17785519]

Wu SL, Fu X, Huang J, Jia TT, Zong FY, Mu SR, Zhu H, Yan Y, Qiu S, Wu Q, Yan W, Peng Y, Chen J, Hui J. Genome-wide analysis of YB-1-RNA interactions reveals a novel role of YB-1 in miRNA processing in glioblastoma multiforme. Nucleic Acids Res. 2015; 43(17):8516–28. [PubMed: 26240386]

Yoon BC, Jung H, Dwivedy A, O'Hare CM, Zivraj KH, Holt CE. Local translation of extranuclear lamin B promotes axon maintenance. Cell. 2012; 148:752–64. [PubMed: 22341447]

Zhang HL, Singer RH, Bassell GJ. Neurotrophin regulation of beta-actin mRNA and protein localization within growth cones. J Cell Biol. 1999; 147(1):59–70. [PubMed: 10508855]

Zivraj KH, Tung YC, Piper M, Gumy L, Fawcett JW, Yeo GS, Holt CE. Subcellular profiling reveals distinct and developmentally regulated repertoire of growth cone mRNAs. J Neurosci. 2010; 30:15464–78. [PubMed: 21084603]

Highlights

- COXIV mRNA zipcode is a nucleation site for formation of axonal trafficking RNPs.
- Zipcode-associated proteins were identified using a proteomics-based approach.
- Approximately 53 proteins are associated with the full-length zipcode.
- FUS and YB-1 were among the zipcode-associated proteins.
- Silencing the expression of FUS and YB-1 reduced axonal levels of COXIV mRNA.

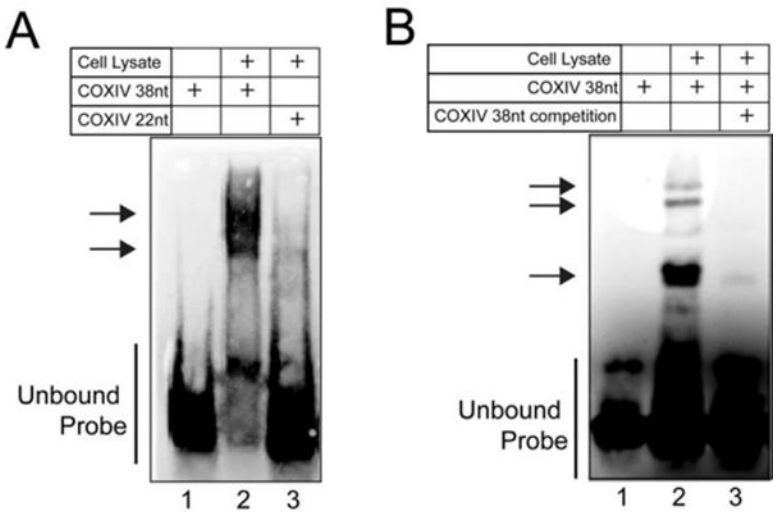

Figure 1. COXIV zipcode serves as a nucleation site for the formation of ribonucleoprotein complexes

3′ biotin-labeled COXIV oligomer probes or 22nt deletion mutant oligomers were incubated with cytosolic proteins derived from 2-week-old retinoic acid-differentiated SHSY5Y cells. After incubation, the complexes were resolved on 4–20% polyacrylamide gels and subsequently visualized using *LightShift Chemiluminescent RNA EMSA kit*. In competitive binding assays, the binding reaction was assembled and carried out in the presence of 100-fold molar excess of non-biotinylated COXIV 38nt probe. (A) Incubation of full-length 38nt COXIV or truncated COXIV probe (COXIV 22nt) with differentiated SHSY5Y cytosolic extract, lane 1, free COXIV 38nt probe; lane 2, gel-shift bands obtained in presence of SHSY5Y cytosolic lysate (2ug), lane 3, gel-shift bands obtained by incubation of truncated COXIV probe (COXIV 22nt) with SHSY5Y cell lysate (2ug) arrows indicate COXIV zipcode-specific gel-shit bands (B) Competition gel-shift assay, lane 1, unbound COXIV 38nt zipcode probe; lane 2 gel shifts observed with the biotinylated COXIV 38nt probe challenged with SHSY5Y cell lysate, lane 3 decreased COXIV band intensity observed with SHSY5Y lysate in the presence of 100-fold excess of unlabeled COXIV 38nt oligomer (specific competitor). Arrows indicate COXIV 38nt dependent gel shift bands. Each experiment consisted of three independent biological replicates (independent lysate preparations). Each experiment was repeated thrice and yielded similar results. (C) Western analyses of COXIV stem-loop RNA oligomer purification from SHSY5Y cytosolic lysates to detect the presence of ZBP-1 in the COXIV zipcode pulldown fraction. The β-actin zipcode (β-actin probe) oligomer affinity purified fractions were used as positive control. Note the absence of the ZBP-1-specific bands in the COXIV 38nt pulldown fraction. Each experiment consisted of three independent lysate preparations and every experiment was conducted three times yielding similar results.

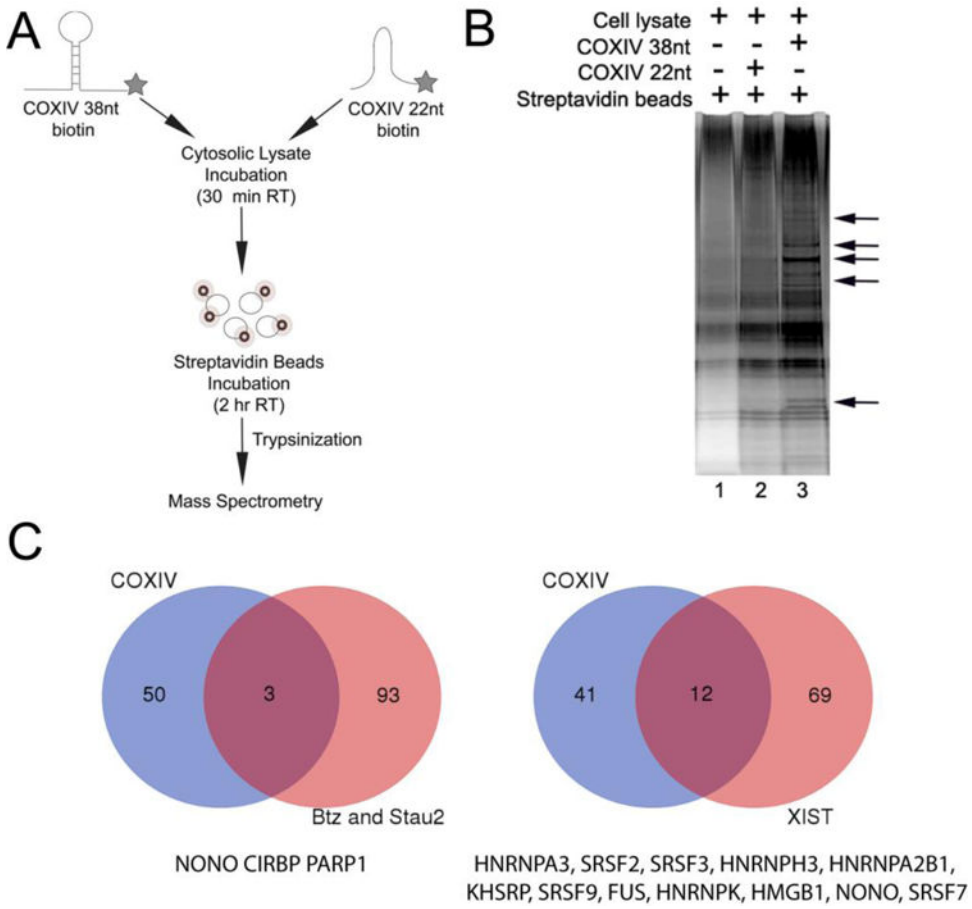

Figure 2. Identification of COXIV 38nt zipcode binding proteins

(A) Schematic of the RNA affinity purification experimental approach employed in these experiments. (B) A representative silver-stained polyacrylamide gel showing the profile of proteins isolated by the COXIV zipcode oligomer affinity purification. Arrows indicate COXIV 38nt-specific protein bands. (C) Venn diagram showing the overlap between the COXIV zipcode affinity purified proteins and those reported in Btz, Stau2 –specific RNA granule and Xist mRNA specific RNA granule proteomic studies (Fritzche et al., 2013 and Chu et al., 2015). The list of common proteins is shown below each diagram.

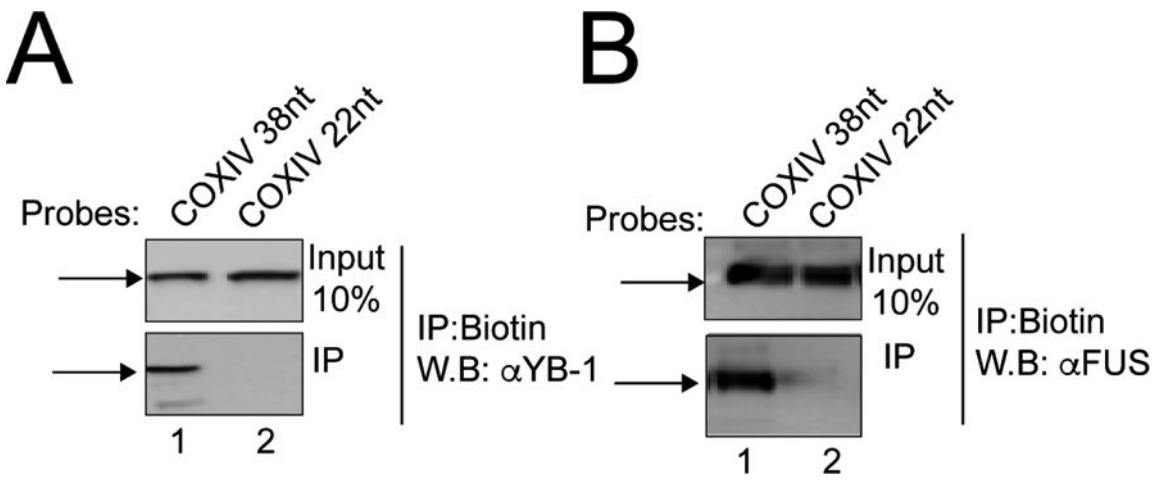

Figure 3. Association of COXIV 38nt zipcode with YB-1, and FUS proteins

Western blot analyses were conducted on COXIV zipcode oligomer affinity purified fractions (lower panel) derived from SHSY5Y cytosolic lysates to detect the presence of candidate proteins (A) YB-1 (B) FUS. A truncated COXIV probe (COXIV 22nt) was used as a control for binding specificity. Arrows indicate antibody-specific immunoreactive bands. Note the presence of antigen in the lysates (upper panel) presented to the biotinylated probes. 10% of the total lysates were applied to the gel. Experiment was repeated thrice with three independent lysate preparations yielding similar results.

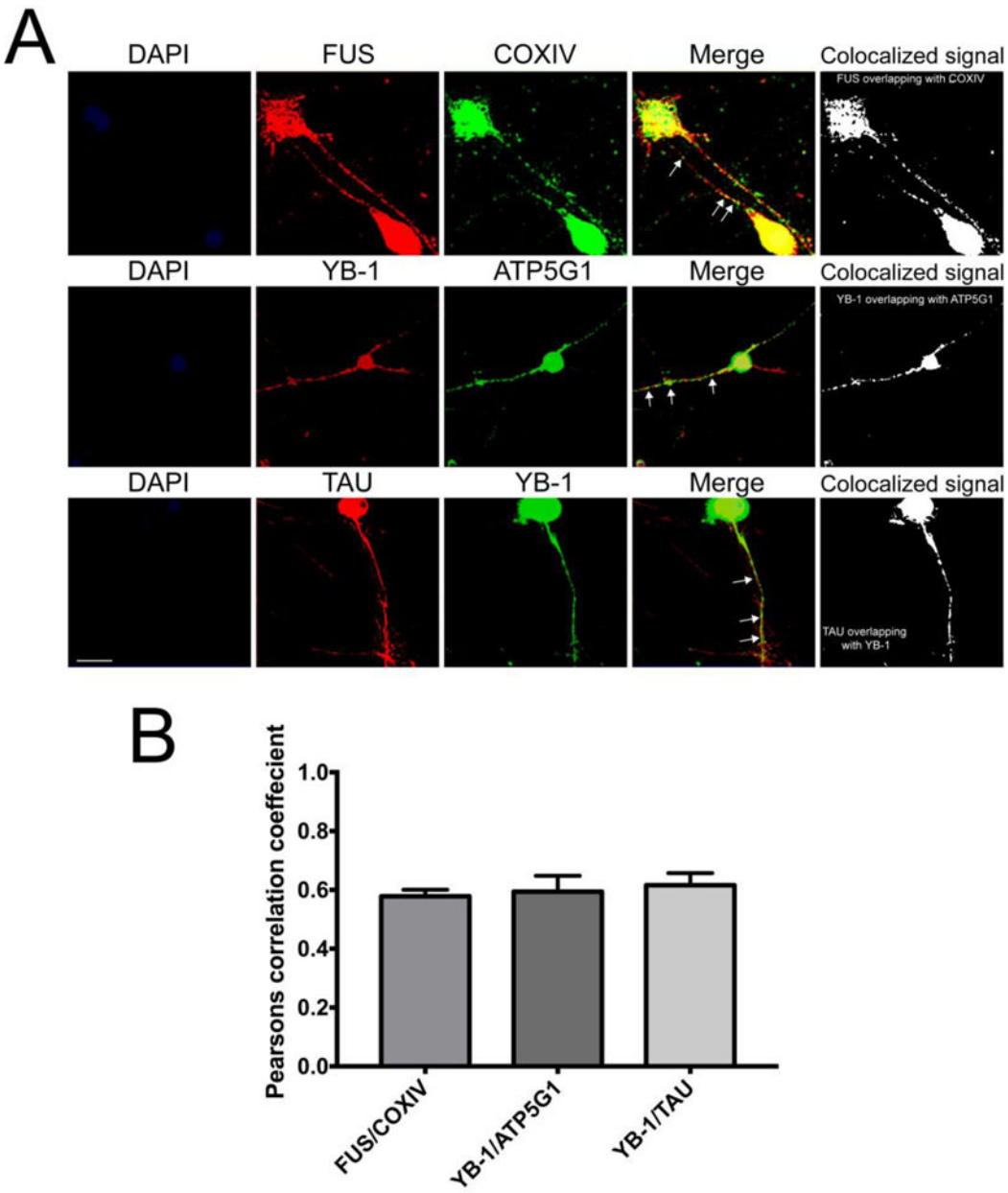

Figure 4. Visualization of FUS, and YB-1 proteins in sympathetic neurons

Immuno-histochemical analyses of dissociated superior cervical ganglion neurons using specific antibodies against FUS (A), YB-1 (B and C). Neurons were co-stained with mitochondrial proteins COXIV, ATP5G1 (A and B, respectively) or cytoskeletal protein Tau (C). The arrows show regions of overlap between the antibody-specific immunostaining. Scale bar 50 μM.

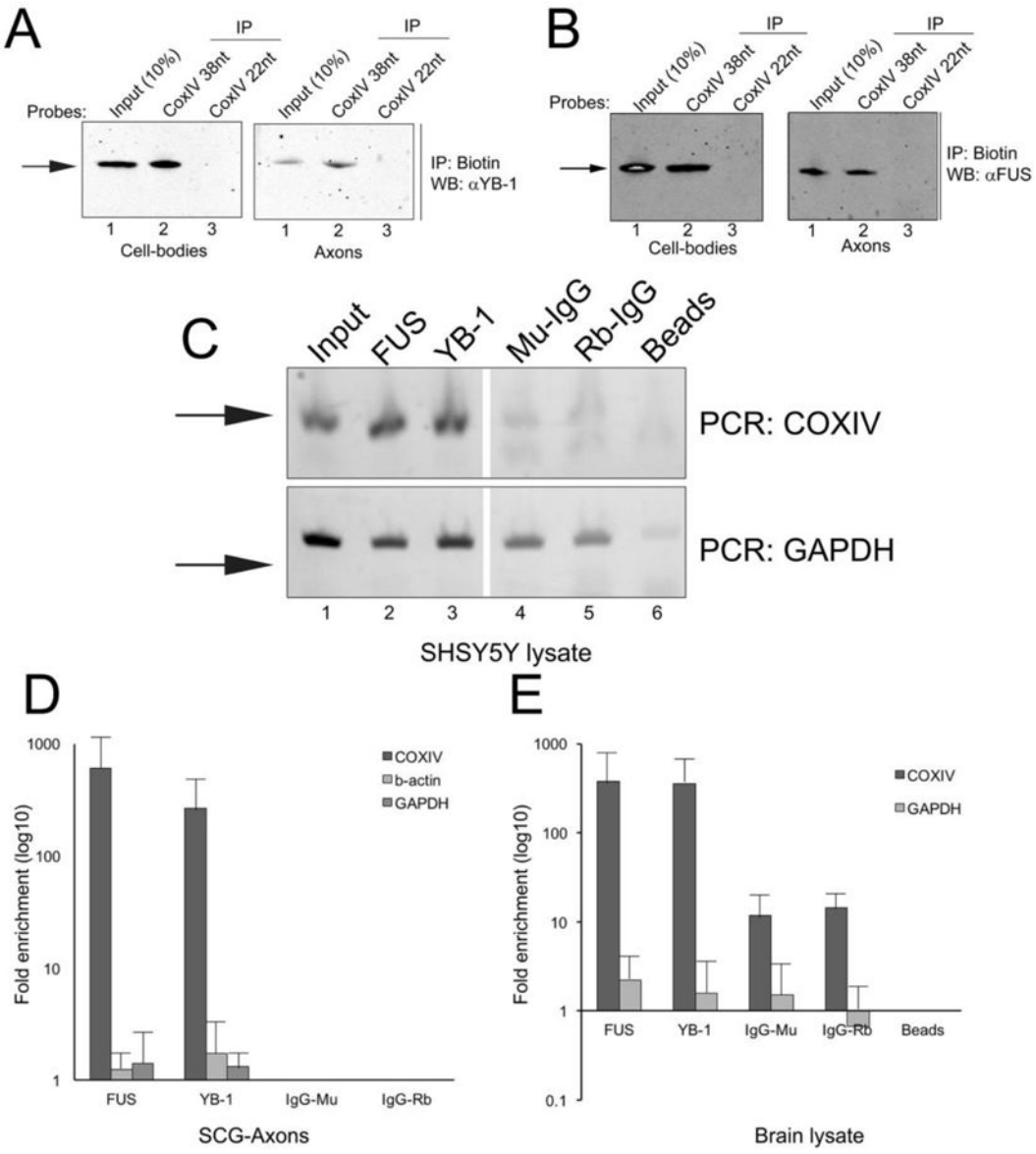

Figure 5. Interaction of COXIV 38nt zipcode and endogenous COXIV mRNA with candidate zipcode binding proteins in SCG lysates

RNA oligomer affinity purifications were performed on cell-body and axonal lysates (A and B) with COXIV 38nt probe and the presence of specific proteins YB-1(A) and FUS(B) was detected using western blot analyses. The truncated COXIV 22nt probe was used as a negative control. Each experiment was repeated three times with similar results. RNA immunoprecipitation assay was performed on SHSY5Y cytosolic fractions (C) axonal lysates (D) or rat brain lysates (E) with FUS-, and YB-1- specific antibodies. Antibodies to the candidate binding proteins were employed to immunopurify RNP complexes and the presence of COXIV mRNA in the RNPs was detected by qRT-PCR. GAPDH mRNA and mouse and rabbit IgG (C–E) as well as β-actin mRNA (E) were used as negative controls. The data are plotted as fold-enrichment relative to mouse or rabbit IgG pulldown for each mRNA (D) or fold-enrichment over protein A beads (E). Values represent mean ± SEM from

three independent experiments. Each experiment consisted three independent lysate preparations.

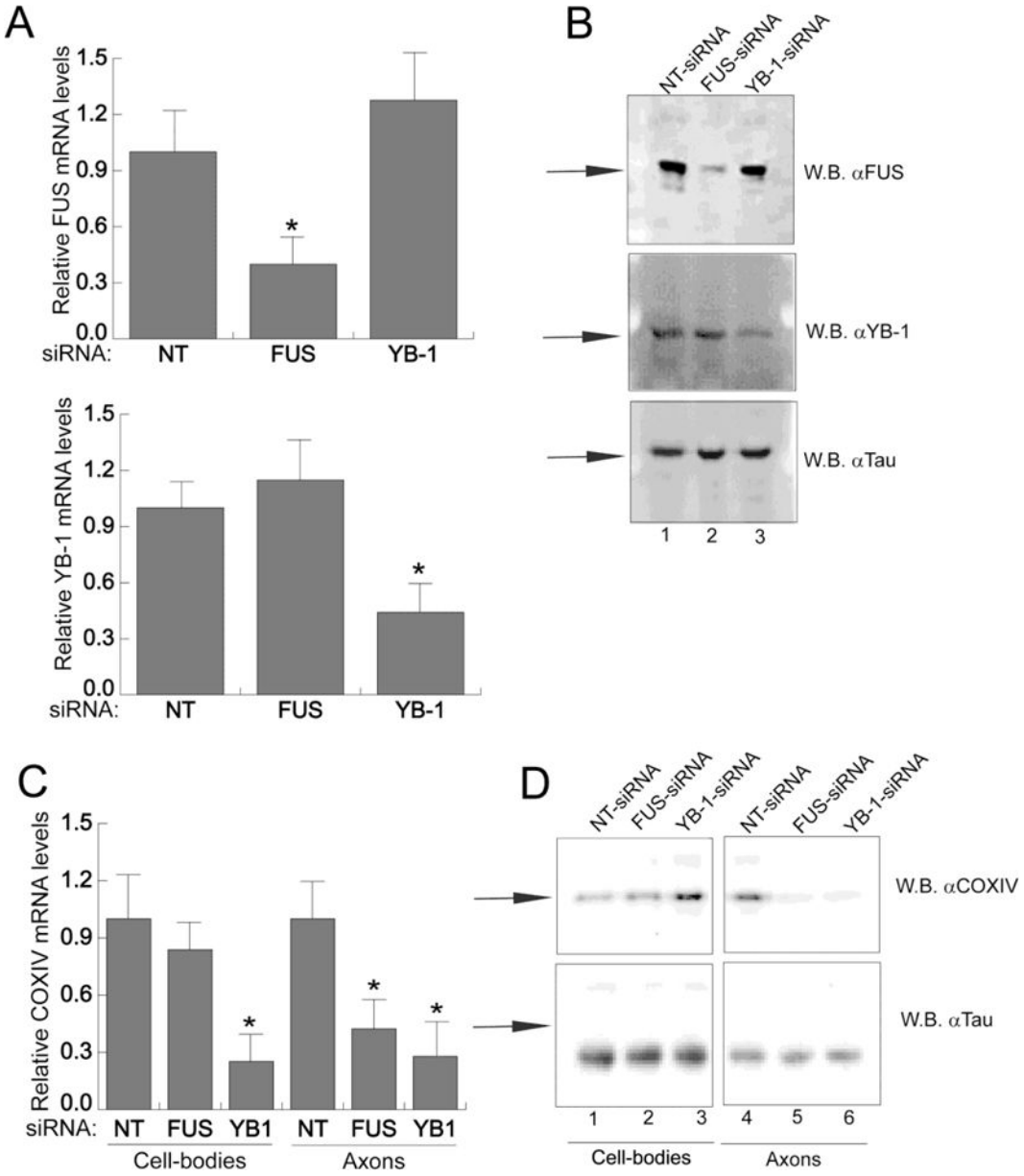

Figure 6. siRNA-mediated knockdown of FUS and YB-1 expression inhibits endogenous COXIV mRNA trafficking and translation in rat sympathetic axons

siRNA oligonucleotides (100pmoles) targeted against either FUS or YB-1 or nontargeting NT-siRNA were transfected into the cell-body compartments of 1-week-old SCG neurons. After transfection (36h), cell-bodies and axonal compartments were lysed and RNA and protein levels were assessed by qRT-PCR and western blot analyses, respectively (A and B). The FUS and YB-1 mRNA levels from cell bodies were measured by qRT-PCR (A) and cell-body protein levels visualized by Western analyses (B). The mRNA levels are expressed relative to RPS18 mRNA, and Tau protein levels served as a loading control for the western analyses. Arrows indicate specific western bands. Values represent mean ± SEM from three

independent experiments. *$p < 0.01$ (one-way ANOVA and post-hoc test). Each experiment was repeated three times with similar results

Table 1

COXIV zipcode interacting proteins identified by RNA affinity purification and mass spectrometry studies.

Accession #	Gene Symbol	# of distinct peptides	% Coverage	Protein Score	Peptides
Q9UII2	ATIF1_HUMAN	4	49.06	131.18	EAGGAFGKR; LQKEIERHK; GSDQSENVDRGAGSIR; EQAEEERYFR
P56385	ATP5I_HUMAN	4	55.1	160.29	YSALFLGVAYGATR; IARELAEDDSILK;VPPVQVSPLIK; ELAEDDSILK
P48047	ATPO_HUMAN	12	48.8	246	FSPLTTNLINLLAENGR; VAASVLNPYVK; SFLSQGQVLKLEAK; QNKLEQVEKELLR; SLNDITAKER; VAASVLNPYVKR; TDPSILGGMIVR; SFLSQGQVLK; VAQILKEPK; LVRPPVQVYGIEGR; FAKLVRPPVQVYGIEGR; ERFSPLTTNLINLLAENGR
Q00535	CDK5_HUMAN	3	10.27	72.68	GLGFCHSR; LADFGLAR; LNATGRDLLQNLLK
Q14011	CIRBP_HUMAN	3	47.67	186.64	SSGGSYRDSYDSYATHNE; SGGYGGSRDYYSSR; YGQISEVVVVKDRETQR
P62633	CNBP_HUMAN	8	53.11	226.71	CGESGHLAKDCDLQEDACYNCGR; DCDLQEDACYNCGR; CGETGHVAINCSK; EQCCYNCGKPGHLAR; CGESGHLAR; SSNECFKCGR; TSEVNCYR; DCDHADEQKCYSCGEFGHIQKDCTK
P14854	CX6B1_HUMAN	3	61.63	99.77	GGDISVCEWYQR; TAPFDSRFPNQNQTR; VYQSLCPTSWVTDWDEQRAEGTFPGKI
P99999	CYC_HUMAN	5	40.95	220.63	KTGQAPGYSYTAANK; TGQAPGYSYTAANKNK; TGQAPGYSYTAANK; KTGQAPGYSYTAANKNK; ADLIAYLK
O43602	DCX_HUMAN	4	11.11	133.46	SFDALLADLTR; SLSDNINLPQGVR; TAHSFEQVLTDITEAIKLETGVVKK; KLYTLDGK
Q86XP3	DDX42_HUMAN	2	4.9	70.75	DILIDPIRVVQGDIGEANEDVTQIVEILHSGPSK; SHFVAASLSNQK
Q7L014	DDX46_HUMAN	2	2.33	85.1	RILSKPIEVQVGGR; LLVATSVAAR
O43143	DHX15_HUMAN	5	13.58	203	SNLGSVVLQLK; HQSFVLVGETGSGK; TLATDILMGVLKEVVR; IRVESLLVTAISK; RGVACTQPR
P25685	DNJB1_HUMAN	5	19.12	122.03	KKQDPPVTHDLR; GASDEEIKR; SIRNEDKILTIEVK; DGSDVIYPAR; SIRNEDKILTIEVK
O14531	DPYL4_HUMAN	7	40.73	258.31	VAVGSDADLVIWNPK; GAPAVVISQGR; NLHQSGFSLSGSQADDHIAR; KTFPDFVYKR; THNLNVEYNIFEGVECR; LLELGITGPEGHVLSHPEEVEAEAVYR; IVNDDQSFYADVHVEDGLIKQIGENLIVPGGIK
Q9BPU6	DPYL5_HUMAN	3	20.39	158.82	THCPIYLVNVSSISAGDVIAAAK; VHAENGELVAEGAKEALDLGITGPEGIEISRPEELEAEATHR; CHGVPLVTISR
O60869	EDF1_HUMAN	6	50	171.8	SKQAILAAQR; GLTQKDLATK; WAAGQNKQHSITK; GKDIGKPIEKGPR; GLTQKDLATKINEKPQVIADYESGR; AIPNNQVLGKIER
P06733	ENOA_HUMAN	5	24.42	244.32	SGETEDTFIADLVVGLCTGQIK; AGAVEKGVPLYR; NFRNPLAK; AVEHINKTIAPALVSK; NVINGGSHAGNK
Q92945	FUBP2_HUMAN	8	13.22	208.42	IGGGIDVPVPR; IINDLLQSLR; HSVGVVIGR; AGLVIGKGGETIKQLQER; IGGDAATTVNNSTPDFGFGGQKR; GGETIKQLQER; GSPQQIDHAK; SVSLTGAPESVQK
P35637	FUS_HUMAN	4	13.31	123.71	AAIDWFDGKEFSGNPIKVSFATR; DQGSRHDSEQDNSDNNTIFVQGLGENVTIESVADYFK; AAIDWFDGKEFSGNPIK; QIGIIKTNKK
P09429	HMGB1_HUMAN	17	73.02	328.76	IKGEHPGLSIGDVAK; KHPDASVNFSEFSK; YEKDIAAYR; GEHPGLSIGDVAK; RPPSAFFLFCSEYRPK; EKYEKDIAAYR; IKGEHPGLSIGDVAKK; HPDASVNFSEFSK; GKPDAAKKGVVK; KGVVKAEK; GKFEDMAKADK; GKGDPKKPR; KHPDASVNFSEFSKK; YEKDIAAYRAK; TYIPPKGETK; LGEMWNNTAADDKQPYEK; FKDPNAPKRPPSAFFLFCSEYRPK; GKFEDMAK; FKDPNAPK
P26583	HMGB2_HUMAN	17	71.77	318.98	KKNEPEDEEEEEEEEDEDEEEEDED; IKSEHPGLSIGDTAK; SEHPGLSIGDTAK; YEKDIAAYR; EKYEKDIAAYR; IKSEHPGLSIGDTAKK; SEAGKKGPGRPTGSK; RPPSAFFLFCSEHRPK; SEHPGLSIGDTAKK; HPDSSVNFAEFSKK; YEKDIAAYRAK; DKQPYEQKAAK; SKFEDMAK; DKQPYEQK; KHPDSSVNFAEFSKK; NYVPPKGDKK
P31942	HNRH3_HUMAN	3	16.76	139.61	STGEAFVQFASK; EIAENALGKHKER; HNGPNDASDGTVR

Accession #	Gene Symbol	# of distinct peptides	% Coverage	Protein Score	Peptides
P61978	HNRPK_HUMAN	6	20.73	193.72	ALRTDYNASVSVPDSSGPER; DLAGSIIGK; DLAGSIIGKGGQR; GSYGDLGGPIITTQVTIPK; GSYGDLGGPIITTQVTIPKDLAGSIIGK; HESGASIKIDEPLEGSEDRIITITGTQDQIQNAQYLLQNSVK
P55145	MANF_HUMAN	2	14.84	103.32	YAPKAASARTDL; LRPGDCEVCISYLGR
P46821	MAP1B_HUMAN	5	7.46	247.04	SVGNTIDPVILFQK; TSDVGGYYYEKIER; SWDTNLIECNLDQELKLFVSR; AIGNIELGIR; TPDTSTYCYETAEKITR
P27816	MAP4_HUMAN	6	9.81	217.03	TAGPIASAQKQPAGK; TTTLSGTAPAAGVVPSR; SVPADLSRPK; TTTAAAVASTGPSSR; LATNTSAPDLKNVR; ASPSKPASAPASR
P40926	MDHM_HUMAN	7	32.84	219.99	AKVAVLGASGGIGQPLSLLLK; TIIPLISQCTPKVDFPQDQLTALTGR; AGAGSATLSMAYAGAR; AKVAVLGASGGIGQPLSLLLKNSPLVSR; LTLYDIAHTPGVAADLSHIETK; NSPLVSRLTLYDIAHTPGVAADLSHIETK
Q15233	NONO_HUMAN	3	11.68	160.31	NLPQYVSNELLEEAFSVFGQVER; AVVIVDDRGR; AAPGAEFAPNKR
Q99497	PARK7_HUMAN	4	35.4	76.89	GAEEMETVIPVDVMR; VTVAGLAGKDPVQCSR; DVVICPDASLEDAKK; EILKEQENR
P09874	PARP1_HUMAN	15	27.32	284.79	VVSEDFLQDVSASTK; TTNFAGILSQGLR; SLQELFLAHILSPWGAEVKAEPVEVVAPR; TLGDFAAEYAK; HASHISKLPK; NTHATTHNAYDLEVIDIFKIER; VVDRDSEEAEIIRK; TAEAGGVTGKGQDGIGSKAEK; SLQELFLAHILSPWGAEVK; VCSTNDLKELLIFNK; SANYCHTSQGDPIGLILLGEVALGNMYELK; SKLPKPVQDLIK; GFSLLATEDKEALKK; AESSDKLYRVEYAK; NREELGFRPEYSASQLK
P62136	PP1A_HUMAN	3	18.79	165.98	SDSEKLNLDSIIGR; AHQVVEDGYEFFAKR; FLHKHDLDLICR
Q9Y5S9	RBM8A_HUMAN	2	7.47	70.14	GRGFGSEEGSR; GFGSEEGSRAR
P22626	ROA2_HUMAN	10	33.99	252.23	YHTINGHNAEVR; RAVAREESGKPGAHVTVK; EESGKPGAHVTVK; YHTINGHNAEVRK; SGRGGNFGFGDSR; GGGGNFGPGPGSNFR; GGGGNFGPGPGSNFRGGSDGYGSGR; GFGFVTFDDHDPVDKIVLQK; AVAREESGKPGAHVTVK; ALSRQEMQEVQSSR
P51991	ROA3_HUMAN	2	18.52	176.61	SSGSPYGGGYGSGGGSGGYGSR; GFAFVTFDDHDTVDKIVVQK
Q9NVA2	SEP11_HUMAN	2	11.35	144.46	SYELQESNVR; AVAVGRPSNEELR
Q15019	SEPT2_HUMAN	8	40.72	266.01	TVQIEASTVEIEER; SKQQPTQFINPETPGYVGFANLPNQVHR; ASIPFSVVGSNQLIEAK; TIISYIDEQFER; GRLYPWGVVEVENPEHNDFLK; AIHNKVNIVPVIAK; GRLYPWGVVEVENPEHNDFLKLR; STLINSLFLTDLYPERVIPGAAEKIER
Q14141	SEPT6_HUMAN	2	8.99	122.18	AATDIARQVGEGCR; SLDDEVNAFKQR
Q16181	SEPT7_HUMAN	3	17.16	173	ILEQQNSSR; STLINSLFLTDLYSPEYPGPSHR; LHEKVNIIPLIAK
Q9UHD8	SEPT9_HUMAN	9	26.28	260.61	SDPAVNAQLDGIISDFEALKR; SITHDIEEKGVR; STLINTLFK; SVQPTSEERIPK; ATVASSTQKFQDLGVKNSEPSAR; RVELSGPKAAEPVSR; THMQNIKDITSSIHFEAYR; FINDQYEKYLQEEVNINR; RTEITIVKPQESAHR
P50454	SERPH_HUMAN	6	24.88	189.89	DQAVENILVSPVVVASSLGLVSLGGK; AVLSAEQLRDEEVHAGLGELLR; HLAGLGLTEAIDKNKADLSR; LFYADHPFIFLVR; GVVEVTHDLQK; SSKQHYNCEHSK
P23246	SFPQ_HUMAN	2	11.66	104.18	NLPQYVSNELLEEAFSVFGQVER; AVVIVDDRGR
Q07955	SRSF1_HUMAN	12	58.47	248.85	SGGGVIRGPAGNNDCR; IYVGNLPPDIR; KLDNTKFR; SHEGETAYIR; TKDIEDVFYK; EAGDVCYADVYRDGTGVVEFVR; YGAIRDIDLK; KEDMTYAVR; FRSHEGETAYIR; GGPPFAFVEFEDPRDAEDAVYGR; TKDIEDVFYKYGAIR; DIEDVFYKYGAIRDIDLK
Q01130	SRSF2_HUMAN	7	32.58	191.23	SYGRPPPDVEGMTSLKVDNLTYR; YGRPPDSHHSR; DRYTKESR; RVFEKYGR; VGDVYIPR; VGDVYIPRDR; TSPDTLRR
P84103	SRSF3_HUMAN	7	57.93	229.06	VYVGNLGNNGNKTELER; VRVELSNGEKR; AFGYYGPLR; VRVELSNGEK; NRGPPPSWGR; NPPGFAFVEFEDPRDAADAVR; NPPGFAFVEFEDPRDAADAVRELDGR
Q13247	SRSF6_HUMAN	7	31.4	209.68	QAGEVTYADAHKER; TNEGVIEFR; ALDKLDGTEINGR; LIVENLSSR; DRDGYSYGSR; RDRDGYSYGSR; TSGRDKYGPPVR

Accession #	Gene Symbol	# of distinct peptides	% Coverage	Protein Score	Peptides
Q16629	SRSF7_HUMAN	4	26.47	197.62	VYVGNLGTGAGKGELER; AFSYYGPLR; NPPGFAFVEFEDPRDAEDAVR; SRFDRPPAR
Q13242	SRSF9_HUMAN	2	11.39	115.96	KLDDTKFR; SHEGETSYIR
P61764	STXB1_HUMAN	7	17.17	213.35	SSASFSTTAVSAR; AAHVFFTDSCPDALFNELVK; HKHIAEVSQEVTR; ISEQTYQLSR; VKEVLLDEDDDLWIALR; LAEQIATLCATLKEYPAVR
Q15785	TOM34_HUM**Hig hlights:** • COXIV mRNA zipcode is a nucleation site for formation of axonal trafficking RNPs. • Zipcode-associate d proteins were identified using a proteomic s-based approach. • Approximately 53 proteins are associated with the full-length zipcode. • FUS and YB-1 were among the zipcode-associated proteins. • Silencing the expressio n of FUS and YB-1 reduced axonal levels of COXIV mRNA. AN	2	8.41	111.68	SSFADISNLLQIEPR; NRVPSAGDVEK
Q12931	TRAP1_HUMAN	2	4.26	63.04	GVVDSEDIPLNLSR; YVAQAHDKPR
P47985	UCRI_HUMAN	3	19.71	100.47	SGPFAPVLSATSR; ESLSGQAVR; GVAGALRPLVQATVPATPEQPVLDLKRPFLSR
P67809	YBOX1_HUMAN	3	24.1	67.89	GAEAANVTGPGGVPVQGSK; NEGSESAPEGQAQQR; AADPPAENSSAPEAEQGGAE

The Table indicates 53 putative COXIV zipcode binding proteins identified by mass spectrometry analyses. The accession number, gene symbol, number of unique peptides identified, percentage of sequence coverage identified from MS/MS data, protein score and a list of sequences are indicated. The protein score according to the analyses software (PEAKS 7; Thermo Scientific) is defined as calculated weighted sum of the −10logP scores of the protein's supporting peptides after removing any redundant peptides. * This asterisk denotes the explanation noted here as a footnote to the table.